Molecular Cytology & Disease

ORIGINAL RESEARCH

Open Access

Inhibition of MiR-30d-5p Promotes Mitochondrial Autophagy and Alleviates Podocyte Injury under High Glucose

Ying Cai [1], Sheng Chen [1], Xiaoli Jiang [1], Qiyuan Wu [1], Bei Guo [1], Fang Wang [1,*]

[1.] Department of Nephrology, Lihuili Hospital, Ningbo Medical Center, 315000 Ningbo, Zhejiang, China

Keywords

MiR-30d-5p

Mitochondrial function

Autophagy

High glucose

Podocyte

* **Correspondence**

Fang Wang

Department of Nephrology, Lihuili Hospital, Ningbo Medical Center, 315000 Ningbo, Zhejiang, China

E-mail: wangffff222@163.com

Received: 1 March 2025

Revised: 29 March 2025

Accepted: 29 April 2025

Published: 30 May 2025

Molecular Cytology & Disease **2025; 1(1): 24-36.**

Abstract

Objective: To study the role of miR-30d-5p in high glucose-induced podocyte injury. **Methods:** Podocytes were hyperglycated with 30 mM glucose, transfected with miR-30d-5p inhibitor and mimic, and then treated with 1 mg/mL 3-MA. The transfection efficiency of miR-30d-5p and the expressions of mitochondrial autophagy related genes (ATG5, PINK1 and PARK2) were detected by qRT-PCR. Apoptosis was detected by flow cytometry. The expressions of LC3I, LC3II, P62, ATG5, PINK1 and PARK2 were measured by Western blotting. JC-1 was used as a fluorescent probe to detect the mitochondrial membrane potential, and Adenosine Triphosphate (ATP) content in cells was quantified by relevant kits. **Results:** In the high glucose-induced podocytes, miR-30d-5p and P62 expressions were upregulated, while ATG5, PINK1, PARK2 and LC3II/LC3I expression levels were downregulated. MiR-30d-5p inhibitor reversed the effect of high glucose on the expressions of ATG5, PINK1, PARK2, LC3I, LC3II and P62. High glucose induced loss of mitochondrial membrane potential and ATP content in podocytes, and increased membrane potential and ATP content were observed after inhibition of miR-30d-5p. **Conclusion:** Inhibition of miR-30d-5p may enhance mitochondrial autophagy by promoting the expressions of ATG5 and PINK1/2, and subsequently alleviate high glucose-induced podocyte damage.

1 Introduction

Diabetes nephropathy (DN) is one of the major microvascular complications of diabetes and the most common reason for the development of end-stage renal disease [1]. The podocyte injury caused by hyperglycemia is one of the development factors of DN [2]. Podocytes are highly specialized terminal differentiated glomerular epithelial cells that play an important role in maintaining the glomerular filtration barrier [3]. Therefore, preventing podocyte injury or promoting podocyte repair is a potential method to treat patients with DN [4]. Moreover, studies have shown that mitochondrial autophagy alleviates mitochondrial damage, which induces podocyte apoptosis, a major risk factor for DN. However, the detailed relationship between mitochondrial function and podocyte injury caused by hyperglycemia remains unclear. Microarray analysis indicated that miRNAs participate in the process of DN and play multiple roles in the pathogenesis of DN, including inflammation, apoptosis, autophagy, and cell proliferation [5,6]. Reportedly, miR-30d-5p is involved in the occurrence of various diseases and is abnormally expressed in patients with attention deficit hyperactivity disorder [7]. It regulates the proliferation and apoptosis of tongue squamous cell carcinoma cells through targeted binding with DLEU2 [8], and can affect the growth and migration of renal tubular epithelial cells induced by transforming growth factor [9]. Previous research found that miR-30d-5p is highly expressed in high glucose-induced podocyte injury. Although increasing evidence suggested that miR-30d-5p can inhibit autophagy in several cell types [10-13], its role in the progression of mitophagy in podocytes remains obscure. Hence, the main purpose of this study is to investigate the effect of miR-30d-5p knockdown on alleviating podocyte injury through mitophagy under high glucose conditions.

2 Materials and methods

2.1 Materials

2.1.1 Cells

Glomerular podocytes MPC5 were purchased from the Shanghai Institute of Chinese Academy of Sciences. The cells were cultured in DMEM medium containing 10% fetal bovine serum, 1% penicillin/streptomycin, and 1×10^4 U/L γ-interferon in a cell incubator at 37 ℃ with 5% CO_2. Cells in the logarithmic growth phase were used for experiments.

2.1.2 Reagents

Primary antibodies against LC3 (ab192890, 14/16 kDa), P62 (ab240635, 62 kDa), ATG5 (ab227084, 32 kDa), PINK1 (ab23707, 66 kDa), PARK2 (ab77924, 55 kDa) and GAPDH (ab8245, 37 kDa), as well as secondary antibodies goat anti-mouse IgG (ab205719) and goat anti-rabbit IgG (ab205718) were procured from Abcam (Cambridge, UK). Mitochondrial membrane potential detection kit (JC-1, C2003S), Adenosine Triphosphate (ATP) detection kit (S0026), and RIPA lysis buffer (P0013B) were obtained from Beyotime (Shanghai, China). Lipofectamine 2000 (11668019) and reverse transcription kit (4366597/K1691) were ordered from Invitrogen (Carlsbad, CA, USA). QuantiTect SYBR Green PCR kit (204145), QIAwave RNA Mini kit (74534), and miRCURY LNA SYBR® Green PCR kit (339345) were provided by Qiagen (Valencia, CA, USA). ECL Western Blotting kit (35055, Thermo Fisher Scientific, Waltham, MA, USA), DMEM high glucose complete medium (PM150210B, Procell, Wuhan, China), and 3-MA (HY-19312, MedChemExpress, Shanghai, China) were prepared.

2.1.3 Instruments

The ABI Prism 7500 Fast Real-Time PCR System was obtained from Applied Biosystems (Foster City, CA, USA), and the GloMax Muti JR Detection System was from Promega (Madison, WI, USA).

2.2 Cell culture

2.2.1 Cell grouping and culture

Podocytes MPC5 were divided into 11 groups: Con group (treatment with 5.5 mM glucose under normal culture conditions), MA-treated group (treatment with 5.5 mM glucose and 24.5 mM mannitol under normal culture conditions), HG-treated group (treatment with 30 mM glucose under normal culture conditions), IC group (transfection with miR-30d-5p inhibitor control and treatment with 30 mM glucose), I group (transfection with miR-30d-5p inhibitor and treatment with 30 mM glucose), I+3-MA-treated group (transfection with miR-30d-5p inhibitor and treatment with 30 mM glucose and autophagy inhibitor (3-MA)), HG-IC+MN group (transfection with miR-30d-5p inhibitor control and mimic control and treatment with 30 mM glucose), I+MN group (transfection with miR-30d-5p inhibitor and miR-30d-5p mimic control and treatment with 30 mM glucose), I+MM group (transfecteion with miR-30d-5p inhibitor and mimic and treatment with 30 mM glucose), I+3-MA+MN (transfection with miR-30d-5p inhibitor and miR-30d-5p mimic control and treatment with 30 mM glucose and 3-MA), I+3-MA+MM group (transfection with miR-30d-5p inhibitor and mimic and treatment with 30 mM glucose and 3-MA).

2.2.2 Cell transfection

The miR-30d-5p inhibitor (I), miR-30d-5p inhibitor control (IC), miR-30d-5p mimic (MM), and miR-30d-5p mimic control (MN) were synthesized by GenePharma Co., Ltd. (Suzhou, China). Lipofectamine 2000 was used for transfection incubation. The transfection efficiency was detected by qRT-PCR. MPC5 cells were seeded in the culture medium and cultured overnight. When the cell confluence reached 80% under the microscope, transfection of I, IC, MM, and MN was initiated. After 48 h of transfection, subsequent treatments were performed.

2.2.3 qRT-PCR

Total RNA was isolated from the MPC5 cell line using the QIAwave RNA Mini kit. RNA was reversely transcribed into cDNA using the reverse transcription kit. qRT-PCR was performed on the ABI Prism 7500 Fast Real-Time PCR System, with the QuantiTect SYBR Green PCR kit or the miRCURY LNA SYBR® Green PCR kit. Relative RNA expression was calculated using the $2^{-\Delta\Delta Ct}$ method, with U6 as the internal reference for miR-30d-5p and GAPDH as the internal reference for ATG5, PINK1, and PARK2. The primer sequences involved are as follows: miR-30d-5p forward primer: 5′-GCGTGTAAACATCCCCGAC-3′; reverse primer: 5′-AGTGCAGGGTCCGAGGTATT-3′. U6 forward primer: 5′-CTCGCTTCGGCAGCAC-3′; reverse primer: 5′-AACGCTTCACGAATTTGCGT-3′. ATG5 forward primer: 5′-CAGACAACGACTGAAAGACCT-3′; reverse primer: 5′-CAGGATCAATAGCAGAAGGACAA-3′. PINK1 forward primer: 5′-GTGGACCATCTGGTTCAACAGG-3′; reverse primer: 5′-GCAGCCAAAATCTGCGATCACC-3′. PARK2 forward primer: 5′-TCGCAACAAATAGTCGGAACAT-3′; reverse primer: 5′-ACACAAGGCAGGGAGTAGC-3′. GAPDH forward primer: 5′-AGAAGGCTGGGGCTCATTTG-3′; reverse primer: 5′-AGGGGCCATCCACAGTCTTC-3′.

2.2.4 Western blotting

Total cell lysates were prepared using RIPA lysis buffer. Proteins were separated by 10% SDS-PAGE gel and then transferred to PVDF membranes. PVDF membranes were blocked with TBST containing 5% skim milk. The blots were then incubated with different primary antibodies overnight at 4 ℃. After incubation with secondary antibodies, bands were detected using the ECL Western Blotting kit and analyzed with LabWorks (TM ver4.6, UVP, BioImaging Systems, NY, USA). GAPDH was used as a control.

2.2.5 Mitochondrial membrane potential detection

Logarithmic phase cells were seeded at 1.5×10^5

cells/well in 6-well plates. After transfection and medium change, cells were cultured for an additional 24 h. The culture medium was removed, and cells were washed twice with PBS. The JC-1 detection kit was applied according to the manufacturer's instructions. Cells were observed and photographed under a fluorescence microscope within 30 min.

2.2.6 ATP content detection

Cellular ATP levels were determined using the firefly luciferase ATP detection kit as per the manufacturer's instructions. Concretely, cells were incubated with PBS, placed in 1.5 mL EP tubes, and kept on ice to prevent enzymatic degradation. Cells were then centrifuged at 1000×g for 5 min at 4 ℃. In a 1.5 mL tube, 100 μL of the supernatant was mixed with 100 μL of the ATP detection working dilution. Luminescence was measured using the GloMax Muti JR Detection System. The protein concentration of each treatment group was determined using the Bradford protein assay. Cellular ATP levels were normalized to the protein content of each sample.

2.2.7 Dual-luciferase reporter assay

The Starbase website (https://starbase.sysu.edu.cn/index.php) was exploited to predict the target genes of miR-30d-5p, and the dual-luciferase reporter assay was performed to verify the targeting relationship between miR-30d-5p and ATG5. Briefly, the wild-type (WT) sequence of ATG5 containing miR-30d-5p binding site or the mutant (MUT) sequence with miR-30d-5p binding site was cloned into the pGL3 luciferase reporter vector to construct WT or MUT luciferase reporter plasmids (WT/MUT-ATG5). MiR-30d-5p mimic and MN were synthesized by GenePharma Co., Ltd. Subsequently, ATG5-WT and ATG5-MUT were co-transfected with miR-30d-5p mimic or MN into podocytes using Lipofectamine 2000 transfection reagent. 48 h later, luciferase activity was measured in each group of cells.

2.2.8 Statistical methods

Quantitative data were described as mean ± standard deviation. Independent sample t-tests were used for Figure 1G, while one-way ANOVA was for multi-group comparisons. All statistical analyses were performed using GraphPad 8.0 software, with $p < 0.05$ considered statistically significant.

3 Results

3.1 High glucose impacted podocyte autophagy-related genes and miR-30d-5p targeted ATG5

After transfection of miR-30d-5p inhibitor into podocytes, the expression of miR-30d-5p in Con, IC, and I groups was detected by qRT-PCR. The results showed that compared with the Con and IC groups, I group displayed significant downregulation of miR-30d-5p, indicating a successful transfection experiment ($p < 0.001$, Figure 1A). Cells were then treated with 30 mM glucose to simulate a high-glucose environment. qRT-PCR was used to detect the expressions of miR-30d-5p and autophagy-related genes under high glucose conditions. The results showed that compared with the Con group, there were no significant differences in the expressions of miR-30d-5p, ATG5, PINK1, and PARK2 in the MA group. However, in the HG group, miR-30d-5p expression was upregulated, while ATG5, PINK1, and PARK2 expressions were downregulated ($p < 0.001$, Figure 1B-E). The binding site of miR-30d-5p on ATG5 is exhibited in Figure 1F, predicting that ATG5 can bind to miR-30d-5p. Additionally, the dual-luciferase reporter assay results indicated that relative to cells transfected with miR-NC and the ATG5-WT reporter plasmid, cells transfected with miR-30d-5p mimic and ATG5-WT had reduced luciferase activity. In two groups with cells transfected with the ATG5-MUT reporter plasmid, there was no difference in luciferase activity, further confirming that ATG5 can bind to miR-30d-5p ($p < 0.001$, Figure 1G).

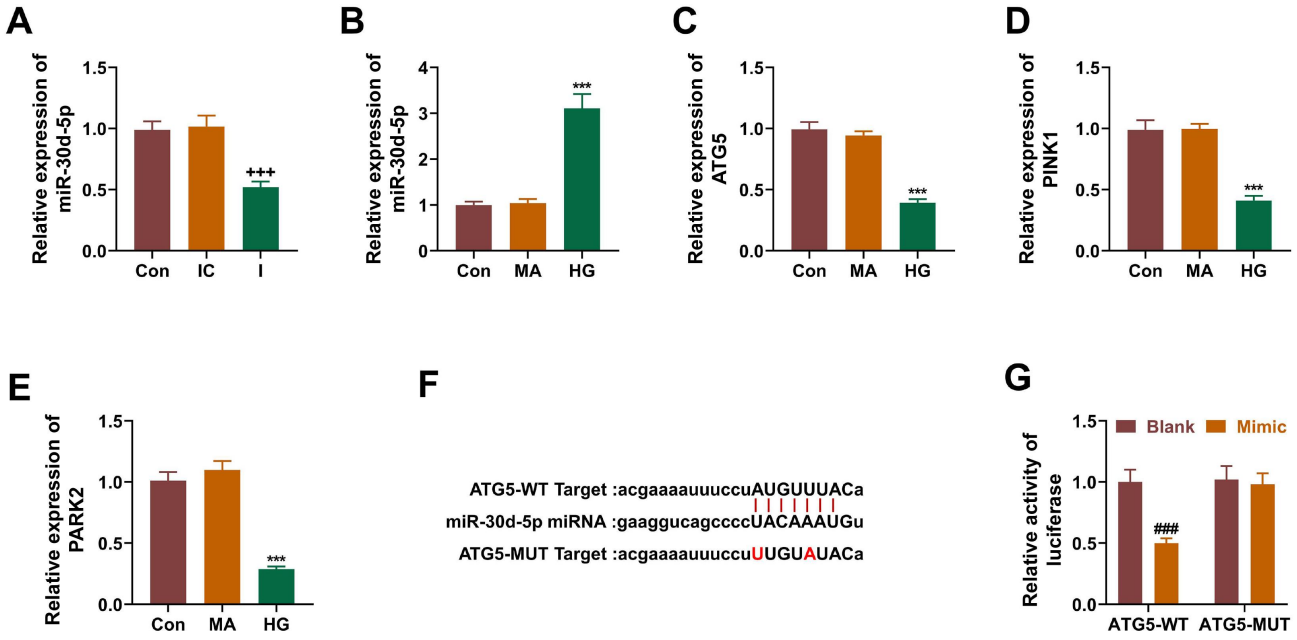

Figure 1 High glucose impacted podocyte autophagy-related genes. (A) qRT-PCR detection of miR-30d-5p transfection efficiency. (B-E) qRT-PCR detection of the expression levels of miR-30d-5p and autophagy-related genes after high-glucose treatment. (F) Prediction of the binding site of miR-30d-5p on ATG5 by Starbase. (G) Dual-luciferase reporter assay to verify the targeting relationship between miR-30d-5p and ATG5. Con: Control group; MA: 5.5 mM glucose and 24.5 mM mannitol treatment group; HG: 30 mM glucose treatment group; ATG5-WT: wild-type ATG5; ATG5-MUT: mutant ATG5. $^{***}p < 0.001$ vs. Con; $^{###}p < 0.001$ vs. Blank; n = 3.

3.2 MiR-30d-5p inhibition affected apoptosis and autophagy in podocytes induced by high glucose

To investigate whether miR-30d-5p affects autophagy in damaged cells, we treated transfected cells with a 3-MA autophagy inhibitor. Firstly, flow cytometry was used to detect apoptosis in each group of cells. The results revealed that high glucose induced an increase in podocyte apoptosis, but inhibition of miR-30d-5p could reverse the effect of high glucose on cell apoptosis. However, autophagy inhibitor 3-MA offset the effect of miR-30d-5p inhibitor on cell apoptosis ($p < 0.001$, Figure 2A-B). Western blotting was further used to detect the expression levels of autophagy-related proteins. High glucose reduced the LC3II/LC3I ratio and promoted P62 expression. MiR-30d-5p inhibitor reversed the effect of high glucose, while 3-MA counteracted the promoting effect of the miR-30d-5p inhibitor on autophagy in podocytes induced by high glucose ($p < 0.001$, Figure 2C-2E).

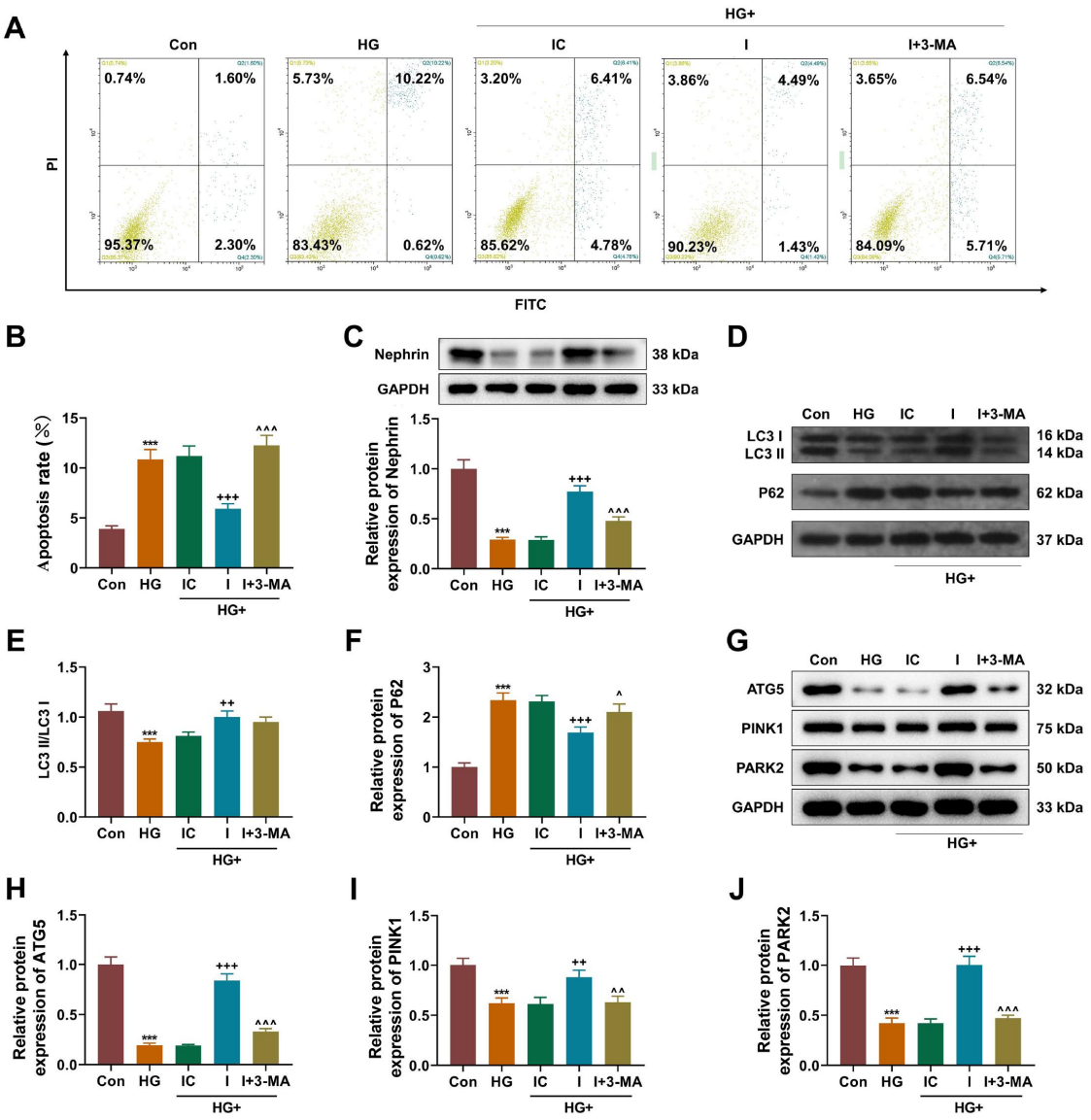

Figure 2 MiR-30d-5p inhibition regulated apoptosis and autophagy in podocytes induced by high glucose. (A-B) Flow cytometry detection of cell apoptosis. (C-E) Western blotting detection of LC3I, LC3II, and P62 protein expression levels. (F-I) Western blotting detection of ATG5, PINK1, and PARK2 protein expression levels. Con: Control group; IC: miR-30d-5p inhibitor control + 30 mM glucose treatment group; I: miR-30d-5p inhibitor + 30 mM glucose treatment group; I+3-MA: miR-30d-5p inhibitor + 30 mM glucose + autophagy inhibitor (3-MA) treatment group. $p < 0.001$ vs. Con; $^{++}p < 0.01$, $^{+++}p < 0.001$ vs. IC; $^{\wedge}p < 0.05$, $^{\wedge\wedge}p < 0.01$, $^{\wedge\wedge\wedge}p < 0.001$ vs. I; n = 3.

3.3 MiR-30d-5p inhibition influenced mitochondrial function in podocytes induced by high glucose

Furthermore, Western blotting was conducted to detect the expressions of mitochondrial associated proteins ATG5, PINK1, and PARK2. The results showed that high glucose increased mitochondrial autophagy related proteins, while miR-30d-5p inhibitor enhanced the occurrence of mitochondrial autophagy in high glucose-induced cells. 3-MA can reverse the effect of miR-30d-5p inhibitor on mitochondrial autophagy related proteins ($p < 0.001$, Figure 2F-2I). JC-1 was used as a fluorescent probe to determine mitochondrial membrane potential in high glucose-induced cells. Red fluorescence indicates mitochondrial membrane potential polarization, while

green fluorescence represents decreased membrane potential. The results unveiled that high glucose triggered mitochondrial membrane potential loss in podocytes. Inhibiting miR-30d-5p in high glucose-induced podocytes increased membrane potential aggregation, and 3-MA reversed such effect of the miR-30d-5p inhibitor ($p < 0.05$, Figure 3A-3B). An detection kit was exploited to measure ATP levels in cells. High glucose reduced ATP levels in podocytes, while miR-30d-5p inhibitor augmented ATP levels in high glucose-induced cells. 3-MA reversed the effect of miR-30d-5p inhibitor ($p < 0.001$, Figure 3C).

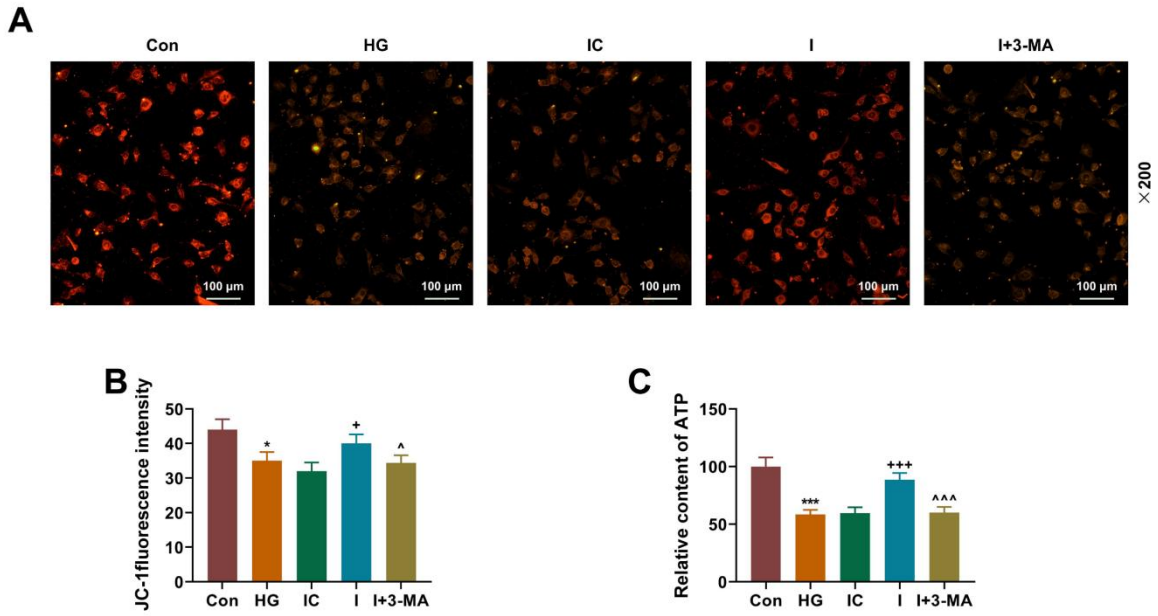

Figure 3 MiR-30d-5p inhibition impacted mitochondrial function in podocytes induced by high glucose. (A-B) JC-1 fluorescence staining to observe mitochondrial membrane potential. (C) ATP detection kit to measure ATP levels. Con: Control group; HG: 30 mM glucose treatment group; IC: miR-30d-5p inhibitor control + 30 mM glucose treatment group; I: miR-30d-5p inhibitor + 30 mM glucose treatment group; I+3-MA: miR-30d-5p inhibitor + 30 mM glucose + autophagy inhibitor (3-MA) treatment group. $p < 0.05$, $p < 0.001$ vs. Con; $^{+}p < 0.05$ vs. IC; $^{\wedge}p < 0.05$, $^{\wedge\wedge\wedge}p < 0.001$ vs. I; n = 3.

3.4 Upregulation of miR-30d-5p attenuated the effects of its inhibitor on apoptosis and autophagy in podocytes induced by high glucose

To further elucidate the role of miR-30d-5p inhibition in high glucose-induced apoptosis and autophagy in podocytes, cells were transfected with miR-30d-5p mimics and/or miR-30d-5p inhibitor. Flow cytometry data unraveled that both miR-30d-5p mimics and 3-MA reversed the reduction in cell apoptosis caused by the miR-30d-5p inhibitor ($p < 0.01$, Figure 4A-4B). Also, miR-30d-5p mimics potentiated the reversal effect of 3-MA on miR-30d-5p inhibitor ($p < 0.05$, Figure 4A-4B). Moreover, Western blotting data further revealed that the increase in LC3II/LC3I ratio and the decrease in P62 expression resulting from miR-30d-5p inhibition were reversed by treatment with miR-30d-5p mimics and 3-MA ($p < 0.001$, Figure 4C-4E). The combined treatment with miR-30d-5p mimics and 3-MA also showed a better reversal effect compared to 3-MA alone ($p < 0.01$, Figure 4C-4E). Collectively, these results indicated that inhibiting miR-30d-5p reduced apoptosis and autophagy in high glucose-induced podocytes.

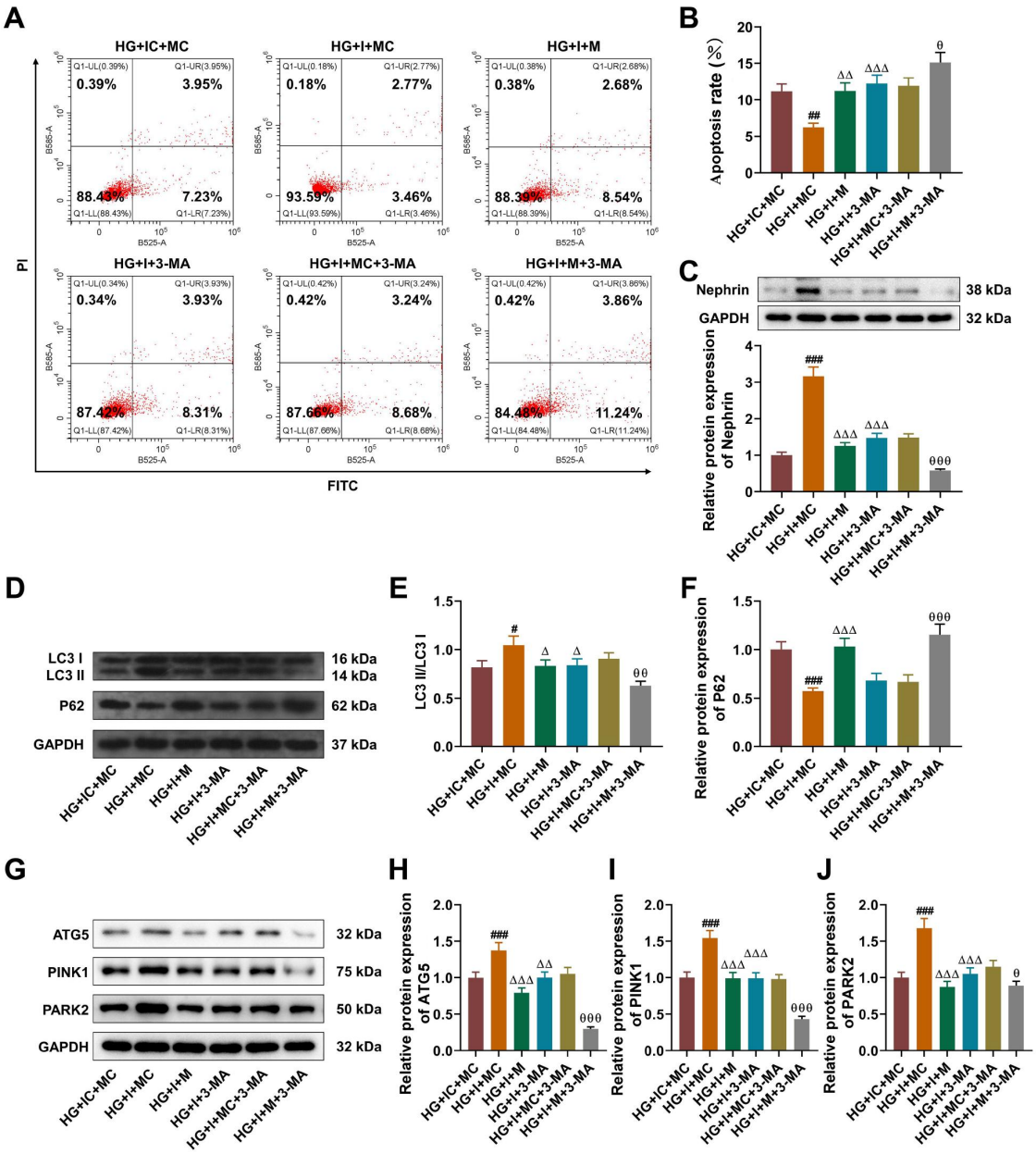

Figure 4 Upregulation of miR-30d-5p reversed the effects of its inhibitor on apoptosis and autophagy in high glucose-induced podocytes. (A-B) Flow cytometry detection of cell apoptosis. (C-E) Western blotting detection of LC3I, LC3II, and P62 protein expression levels. (F-I) Western blotting detection of ATG5, PINK1, and PARK2 protein expression levels. HG-IC+MN: miR-30d-5p inhibitor control and mimic control + 30 mM glucose treatment group; I+MN: miR-30d-5p inhibitor and miR-30d-5p mimic control + 30 mM glucose treatment group; I+MM: miR-30d-5p inhibitor and mimic + 30 mM glucose treatment group; I+3-MA: miR-30d-5p inhibitor + 30 mM glucose and 3-MA treatment group; I+3-MA+MN: miR-30d-5p inhibitor and miR-30d-5p mimic control + 30 mM glucose and 3-MA treatment; I+3-MA+MM: miR-30d-5p inhibitor and mimic + 30 mM glucose and 3-MA treatment. $^{\#}p < 0.05$, $^{\#\#}p < 0.01$, $^{\#\#\#}p < 0.001$ vs. HG-IC+MN; $^{\triangle}p < 0.05$, $^{\triangle\triangle}p < 0.01$, $^{\triangle\triangle\triangle}p < 0.001$ vs. I+MN; $^{\theta}p < 0.05$, $^{\theta\theta}p < 0.01$, $^{\theta\theta\theta}p < 0.001$ vs. I+3-MA+MN; n = 3.

3.5 Upregulation of miR-30d-5p offset the effects of its inhibitor on mitochondrial function changes in high glucose-induced podocytes

The expressions of mitochondrial related proteins ATG5, PINK1, and PARK2 were analyzed. Results showed that the promotion of mitochondrial

autophagy by the miR-30d-5p inhibitor in high glucose-induced cells was reversed by 3-MA and miR-30d-5p mimics (p < 0.001, Figure 4F-4I). Moreover, the combined treatment with 3-MA and miR-30d-5p mimics showed a better reversal effect compared to 3-MA alone (p < 0.001, Figure 4F-4I). JC-1 was used as a fluorescent probe to detect mitochondrial membrane potential in high glucose-induced cells. The data indicated that inhibiting miR-30d-5p in high glucose-induced podocytes increased membrane potential aggregation, which was reversed by 3-MA and miR-30d-5p mimics (p < 0.05, Figure 5A-5B). Additionally,miR-30d-5p mimics strengthened the reversal effect of 3-MA (p < 0.01, Figure 5A-5B). ATP levels in cells were measured using an ATP detection kit. The upregulation of ATP triggered by miR-30d-5p inhibitor was reversed after treatment with 3-MA and miR-30d-5p mimics (p < 0.01, Figure 5C-D), and the combined treatment showed a more significant reversal effect on ATP levels compared to 3-MA alone (p < 0.05, Figure 5C-D). Collectively, these results demonstrated that inhibiting miR-30d-5p promoted mitochondrial autophagy in high glucose-induced cells.

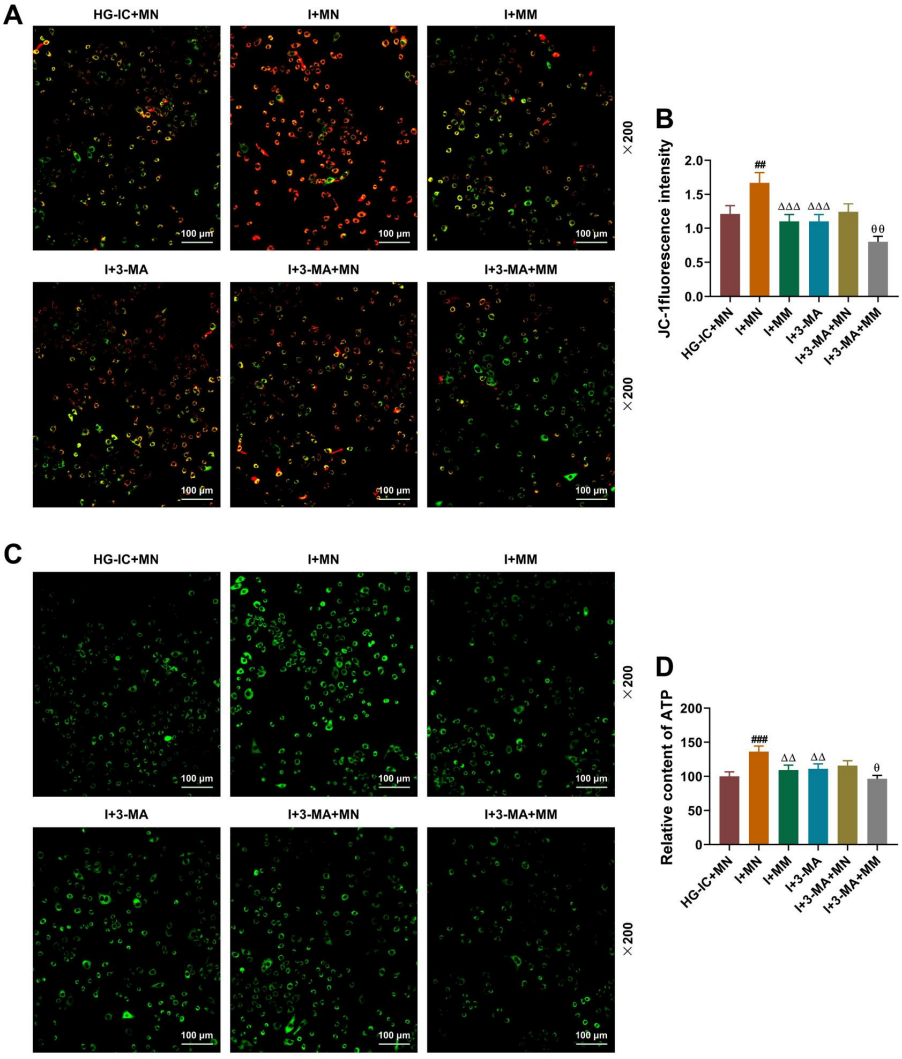

Figure 5 Upregulation of miR-30d-5p attenuated the effects of its inhibitor on mitochondrial function changes in high glucose-induced podocytes. (A-B) JC-1 fluorescence staining to observe mitochondrial membrane potential. (C-D) ATP detection kit to measure ATP levels. HG-IC+MN: miR-30d-5p inhibitor control and mimic control + 30 mM glucose treatment group; I+MN: miR-30d-5p inhibitor and miR-30d-5p mimic control + 30 mM glucose treatment group; I+MM: miR-30d-5p inhibitor and mimic + 30 mM glucose treatment group; I+3-MA:

miR-30d-5p inhibitor + 30 mM glucose and 3-MA treatment group; I+3-MA+MN: miR-30d-5p inhibitor and miR-30d-5p mimic control + 30 mM glucose and 3-MA treatment; I+3-MA+MM: miR-30d-5p inhibitor and mimic + 30 mM glucose and 3-MA treatment. $^{\#\#}p < 0.01$, $^{\#\#\#}p < 0.001$ vs. HG-IC+MN; $^{\triangle\triangle}p < 0.01$, $^{\triangle\triangle\triangle}p < 0.001$ vs. I+MN; $^{\Theta}p < 0.05$, $^{\Theta\Theta}p < 0.01$ vs. I+3-MA+MN; n = 3.

4 Discussion

Mitochondrial dysfunction is one of the reasons for the occurrence and development of DN and other glomerular diseases. Therefore, mitigating mitochondrial dysfunction is instrumental in the treatment of DN. More and more evidence confirmed that podocyte autophagy induced by high glucose contributes to the treatment of DN and the control of glomerular diseases [14]. Podocyte autophagy is mainly responsible for the degradation of proteins and organelles, thereby regulating cellular homeostasis, and autophagy disorder is considered an important inducer of podocyte injury. Studies have reported that increased autophagy has a cytoprotective effect on podocyte injury induced by antibodies and interferon-α in lupus nephritis [15-18]. Moreover, mitophagy is a vital mechanism for clearing damaged mitochondria and maintaining intracellular stability [19]. ATG5 is a gene involved in the initiation of autophagy [20]. The PINK1/Parkin signaling pathway, as an important molecular mechanism regulating mitochondrial autophagy, may be associated with glomerular podocyte injury [21]. Reportedly, ATG5 silencing inhibits autophagy and triggers podocyte apoptosis. High glucose regulates the ROS/PINK1/Parkin signaling pathway to induce apoptosis in retinal pigment epithelial cells and suppress mitochondrial autophagy [22,23]. MitoTEMPO protects podocytes from injury by inhibiting the NLRP3 inflammasome through PINK1/Parkin pathway-mediated mitophagy [24]. Studies have also shown that inhibiting the PINK1-PRKN pathway to promote mitochondrial dynamics can alleviate DN [25]. Herein, we found that compared with the control, the expressions of ATG5 and PINK1/2 were markedly downregulated in podocytes treated with high glucose. ATG5 and PINK1/2 are related to mitophagy, and knocking out ATG5 and PINK1 can inhibit the formation of autophagosomes and mitophagy [26,27]. When autophagy is activated, conversion from LC3I to LC3II can be observed [28]. It has been documented that rapamycin promotes the initiation of autophagic flux and increases the conversion from LC3I to LC3II in the glomerulus [29]. In addition, some research has shown that ursolic acid reduces podocyte mitotic mutation via inhibiting the accumulation of autophagy P62 in DN [30]. Both diabetic mice and podocytes treated with high glucose exhibit mitochondrial structural and functional abnormalities, further damaging podocytes [31]. Our study found that high glucose decreased LC3II/LC3I ratio, promoted P62 expression, and induced podocyte apoptosis, indicating that autophagy may be inhibited in high glucose-induced podocyte mitochondria.

Current studies indicated that increased gene activity can prevent diabetes-induced podocyte injury and effectively alleviate the progression of DN [32,33]. Long non-coding RNA X-inactive specific transcript (lncRNA XIST) alleviates diabetic peripheral neuropathy by inducing autophagy through the miR-30d-5p/SIRT1 axis [34]. Besides, miR-30d-5p inhibits RCC cell proliferation and autophagy by targeting ATG5, and this pathway may provide a reference for the design of new cancer therapies [10]. Herein, we observed a significant increase in miR-30d-5p expression in podocytes treated with high glucose compared to the control, hinting a certain correlation between miR-30d-5p and high glucose-induced podocyte injury. Contrary to our research results, Huang et al. proved that the expression of miR-30d-5p is downregulated in diabetes model mice [35]. We speculate that the

discrepancy may be due to differences in experimental models, so we may choose animal models to further verify the results of this study in the future. Moreover, autophagy can protect podocytes from apoptosis [36]. XIST promotes podocyte autophagy via waning miR-30d-5p, thereby preventing podocyte apoptosis [37]. Our results indicated that inhibiting miR-30d-5p promoted autophagy in damaged cells and reduced podocyte apoptosis, which was reversed by 3-MA. This further confirmed that inhibiting miR-30d-5p can promote mitophagy in high glucose-induced cells and dampen podocyte apoptosis.

The changes in mitochondrial membrane potential and ATP indicate the degree of mitochondrial damage [33]. The results of this study unveiled that high glucose-induced podocytes exhibit an increase in monomers, loss of membrane potential, and a decrease in ATP content. Inhibition of miR-30d-5p increased polymerization and upregulated ATP, and 3-MA reversed the inhibitory effect of miR-30d-5p. The comprehensive results demonstrated that miR-30d-5p can regulate high glucose-induced mitochondrial damage and autophagy by repressing autophagy related genes. Intriguingly, studies have shown that lactate dehydrogenase A, a direct target of miR-30d-5p, can promote the Warburg effect to produce lactate and ATP under aerobic conditions [38]. Therefore, we speculated that miR-30d-5p inhibition may increase ATP content through the action of lactate dehydrogenase A, thereby affecting autophagy. However, this hypothesis requires further experimental validation. Furthermore, there are limitations in our study. First, the experimental design did not include an equivalent osmotic control group. Second, the role of miR-30d-5p was only explored in high glucose-induced podocytes, and further validation in animal experiments is needed to elucidate its role and regulatory mechanisms in DN.

In conclusion, inhibition of miR-30d-5p in high glucose-induced podocytes may promote ATG5 to boost mitochondrial autophagy and alleviate podocyte injury. MiR-30d-5p may be a new target for the treatment of DN, which provides a new insight for the treatment.

Acknowledgements

Not applicable.

Conflicts of Interest

All authors declare that the research was conducted in the absence of any commercial or fnancial relationships that could be construed as a potential confict of interest.

Author Contributions

Conceptualization: Y.C.; Data curation: S.C.; Formal analysis: X.J.; Methodology: Q.W.; Writing – original draft: B.G.; Writing – review and editing: F.W.; All authors have read and agreed to the published version of manuscript.

Funding

This work was supported by the Ningbo Natural Science Foundation (No. 2021J282).

Availability of Data and Materials

The original contributions presented in the study are included in the article, further inquiries can be directed to the corresponding authors.

Supplementary Materials

Not applicable.

References

[1] Xiong Y, Zhou L. The Signaling of Cellular Senescence in Diabetic Nephropathy. *Oxidative Medicine and Cellular Longevity* 2019; 2019: 7495629.

[2] Ke G, Chen X, Liao R, et al. Receptor activator of NF-κB mediates podocyte injury in diabetic nephropathy. *Kidney International* 2021; 100(2): 377-390.

[3] Luo Q, Liang W, Ding GH. Research progress of mTOR

signaling in the podocyte injury of diabetic kidney disease. *Chinese Journal of Nephrology* 2022; 38(7): 639-643.

[4] Liu YR, Yang NJ, Zhao ML, et al. Hypericum perforatum L. Regulates Glutathione Redox Stress and Normalizes Ggt1/Anpep Signaling to Alleviate OVX-Induced Kidney Dysfunction. *Frontiers in Pharmacology* 2021; 12: 628651.

[5] McClelland A, Hagiwara S, Kantharidis P. Where are we in diabetic nephropathy: microRNAs and biomarkers? *Current Opinion in Nephrology and Hypertension* 2014; 23(1): 80-86.

[6] Yarahmadi A, Shahrokhi SZ, Mostafavi-Pour Z, et al. MicroRNAs in diabetic nephropathy: From molecular mechanisms to new therapeutic targets of treatment. *Biochemical Pharmacology* 2021; 189: 114301.

[7] Sun JW, Zhang F, Zhu P, et al. Analysis of the role of miR-30d-5p in the pathogenesis of attention deficit hyperactivity disorder based on bioinformatics. *Journal of Psychiatry* 2020; 33(2): 6.

[8] Fu J, Li N, Yuan QM. The molecular mechanism by which DLEU2 targets miR-30d-5p to affect the proliferation and apoptosis of tongue squamous cell carcinoma cells. *Chinese Journal of Gerontology* 2021; 41(20): 6.

[9] Chen XW, Liao XP, Li SM, et al. Effects of miR-30d-5p on TGF- β 1-induced growth and migration of renal tubular epithelial cells. *Journal of Medical Postgraduates* 2020; 33(12): 1239-1245.

[10] Liang L, Yang Z, Deng Q, et al. miR-30d-5p suppresses proliferation and autophagy by targeting ATG5 in renal cell carcinoma. *FEBS Open Bio* 2021; 11(2): 529-540.

[11] Xu Q, Guohui M, Li D, et al. lncRNA C2dat2 facilitates autophagy and apoptosis via the miR-30d-5p/DDIT4/mTOR axis in cerebral ischemia-reperfusion injury. *Aging* 2021; 13(8): 11315-11335.

[12] Zhao F, Qu Y, Zhu J, et al. miR-30d-5p Plays an Important Role in Autophagy and Apoptosis in Developing Rat Brains After Hypoxic-Ischemic Injury. *Journal of Neuropathology and Experimental Neurology* 2017; 76(8): 709-719.

[13] Jiang M, Wang H, Jin M, et al. Exosomes from MiR-30d-5p-ADSCs Reverse Acute Ischemic Stroke-Induced, Autophagy-Mediated Brain Injury by Promoting M2 Microglial/Macrophage Polarization. *Cellular Physiology and Biochemistry* 2018; 47(2): 864-878.

[14] Fan Y, Yang Q, Yang Y, et al. Sirt6 Suppresses High Glucose-Induced Mitochondrial Dysfunction and Apoptosis in Podocytes through AMPK Activation. *International Journal of Biological Sciences* 2019; 15(3): 701-713.

[15] Qi YY, Zhou XJ, Cheng FJ, et al. Increased autophagy is cytoprotective against podocyte injury induced by antibody and interferon-α in lupus nephritis. *Annals of the Rheumatic Diseases* 2018; 77(12): 1799-1809.

[16] Lu Q, Hou Q, Cao K, et al. Complement factor B in high glucose-induced podocyte injury and diabetic kidney disease. *JCI Insight* 2021; 6(19).

[17] Jiang L, Cui H, Ding J. Smad3 signalling affects high glucose-induced podocyte injury via regulation of the cytoskeletal protein transgelin. *Nephrology* 2020; 25(9): 659-666.

[18] Luo J, Jiang J, Huang H, et al. C-peptide ameliorates high glucose-induced podocyte dysfunction through the regulation of the Notch and TGF- β signaling pathways. *Peptides* 2021; 142: 170557.

[19] Al-Waili N, Al-Waili H, Al-Waili T, et al. Natural antioxidants in the treatment and prevention of diabetic nephropathy; a potential approach that warrants clinical trials. *Redox Report* 2017; 22(3): 99-118.

[20] Cao S, Hung YW, Wang YC, et al. Glutamine is essential for overcoming the immunosuppressive microenvironment in malignant salivary gland tumors. *Theranostics* 2022; 12(13): 6038-6056.

[21] Lu W, Yu L. Research progress on mitophagy of glomerular podocytes and the PINK1/Parkin signaling pathway. *Chinese Journal of Nephrology* 2017; 33(4): 309-312.

[22] Seong SB, Ha DS, Min SY, Ha TS. Autophagy Precedes Apoptosis in Angiotensin II-Induced Podocyte Injury. *Cellular Physiology and Biochemistry* 2019; 53(5): 747-759.

[23] Zhang Y, Xi X, Mei Y, et al. High-glucose induces retinal pigment epithelium mitochondrial pathways of apoptosis and inhibits mitophagy by regulating ROS/PINK1/Parkin signal pathway. *Biomedicine & Pharmacotherapy* 2019; 111: 1315-1325.

[24] Liu B, Wang D, Cao Y, et al. MitoTEMPO protects against podocyte injury by inhibiting NLRP3 inflammasome via PINK1/Parkin pathway-mediated mitophagy. *European Journal of Pharmacology* 2022; 929: 175136.

[25] Zhu JY, van de Leemput J, Han Z. Promoting mitochondrial dynamics by inhibiting the PINK1-PRKN pathway to relieve diabetic nephropathy. *Disease Models & Mechanisms* 2024; 17(4): dmm050471.

[26] Murphy KR, Baggett B, Cooper LL, et al. Enhancing

Autophagy Diminishes Aberrant Ca2+ Homeostasis and Arrhythmogenesis in Aging Rabbit Hearts. *Frontiers in Physiology* 2019; 10: 1277.

[27] Gao Z, Yi W, Tang J, et al. Urolithin A protects against acetaminophen-induced liver injury in mice via sustained activation of Nrf2. *International Journal of Biological Sciences* 2022; 18(5): 2146-2162.

[28] Cao Y, Chen J, Ren G, et al. Punicalagin Prevents Inflammation in LPS-Induced RAW264.7 Macrophages by Inhibiting FoxO3a/Autophagy Signaling Pathway. *Nutrients* 2019; 11(11): 2794.

[29] Ji J, Zhao Y, Na C, et al. Connexin 43-autophagy loop in the podocyte injury of diabetic nephropathy. *International Journal of Molecular Medicine* 2019; 44(5): 1781-1788.

[30] Mei H, Jing T, Liu H, et al. Ursolic Acid Alleviates Mitotic Catastrophe in Podocyte by Inhibiting Autophagic P62 Accumulation in Diabetic Nephropathy. *International Journal of Biological Sciences* 2024; 20(9): 3317-3333.

[31] Guo Y, Wang M, Liu Y, et al. BaoShenTongLuo formula protects against podocyte injury by regulating AMPK-mediated mitochondrial biogenesis in diabetic kidney disease. *Chinese Medicine* 2023; 18(1): 32.

[32] Wu L, Wang Q, Guo F, et al. Involvement of miR-27a-3p in diabetic nephropathy via affecting renal fibrosis, mitochondrial dysfunction, and endoplasmic reticulum stress. *Journal of Cellular Physiology* 2021; 236(2): 1454-1468.

[33] Hong Q, Zhang L, Das B, et al. Increased podocyte Sirtuin-1 function attenuates diabetic kidney injury. *Kidney International* 2018; 93(6): 1330-1343.

[34] Liu BY, Li L, Bai LW, Xu CS. Long Non-coding RNA XIST Attenuates Diabetic Peripheral Neuropathy by Inducing Autophagy Through MicroRNA-30d-5p/sirtuin1 Axis. *Frontiers in Molecular Biosciences* 2021; 8: 655157.

[35] Huang D, Yang B, Wang LM, et al. Danhong injection represses diabetic retinopathy and nephropathy advancement in diabetic mice by upregulating microRNA-30d-5p and targeting JAK1. *Bioengineered* 2022; 13(4): 8187-8200.

[36] Su Y, Yao S, Zhao S, et al. LncRNA CCAT1 functions as apoptosis inhibitor in podocytes via autophagy inhibition. *Journal of Cellular Biochemistry* 2020; 121(1): 621-631.

[37] Cai Y, Chen S, Jiang X, et al. LncRNA X Inactive Specific Transcript Exerts a Protective Effect on High Glucose-Induced Podocytes by Promoting the Podocyte Autophagy via miR-30d-5p/BECN-1 Axis. *International Journal of Endocrinology* 2023; 2023: 3187846.

[38] He Y, Chen X, Yu Y, et al. LDHA is a direct target of miR-30d-5p and contributes to aggressive progression of gallbladder carcinoma. *Molecular Carcinogenesis* 2018; 57(6): 772-783.